The Extracellular Matrix of *Xenopus laevis* Eggs: A Quick-Freeze, Deep-Etch Analysis of Its Modification at Fertilization

Carolyn A. Larabell and Douglas E. Chandler

Department of Zoology, Arizona State University, Tempe, Arizona 85287

Abstract. Eggs of the amphibian, *Xenopus laevis*, were quick-frozen, deep-etched, and rotary-shadowed. The structure of the extracellular matrix surrounding these eggs, including the perivitelline space and the vitelline envelope (VE), was visualized in platinum replicas by electron microscopy. The perivitelline space contains an elaborate filamentous glycocalyx which connects microvillar tips to the plasma membrane, to adjacent microvilli, and to the overlying VE. The VE is comprised of two layers, the innermost of which is a thin network of horizontal fibrils lying on the tips of the microvilli. The outermost is a thicker layer of large, cable-like fibers which twist and turn throughout the envelope. Upon fertilization, three dramatic modifications of the matrix occur. A thin sheet of smooth material, termed the smooth layer, is deposited on the tips of the microvilli and separates the egg from the overlying envelopes. The VE above is transformed from a thick band of cable-like fibers to concentric fibrous sheets, the altered VE. Finally, an ornate band of particles, corresponding to the fertilization layer in previous studies, is deposited at the altered VE/jelly interface. The altered VE and the fertilization layer comprise the fertilization envelope, which effects the structural block to polyspermy.

MATURE eggs of many species exhibit a highly organized extracellular matrix (ECM)[1] that is securely attached to the cell surface. These matrices (e.g., the vitelline layer in sea urchin eggs and the zona pellucida in mammalian eggs) are filamentous in structure and contain glycoprotein sperm receptors which facilitate sperm binding (Glabe and Vacquier, 1978; Bleil and Wassarman, 1980; Rossignol et al., 1984). Upon fertilization, cortical granule secretions interact with these egg investments to produce a chemically and structurally altered matrix which prevents further sperm entry and the possibility of abnormal development (Barros and Yanagimachi, 1971, 1972; Grey et al., 1974, 1976; Veron et al., 1977; Chandler and Heuser, 1980; Gerton and Hedrick, 1986). Thus, eggs represent an excellent model for analyzing ECM structural dynamics that are paralleled by a change in biological function.

The ECM of amphibians has been best studied in the South African clawed frog, *Xenopus laevis*. The unfertilized *Xenopus* egg is surrounded by the perivitelline space (PS) and vitelline envelope (VE). The PS, as seen in thin sections, is a 1-μm-thick area between the cell surface and overlying VE and contains a glycocalyx-like, filamentous material as well as clusters of small, membrane-bound vesicles (Grey et al., 1974). The VE, also ~1 μm thick, is a loose network of filaments ~4–7 nm in diameter arranged in alternating layers or bundles (Grey et al., 1974). The VE consists of 85% protein and 15% sugar (Wolf et al., 1976), and gel electrophoresis reveals seven proteins with estimated molecular masses of 120, 112, 69, 64, 57, 41, and 37 kD, all of which are glycosylated except for the 57-kD protein (Gerton and Hedrick, 1986).

Fusion of a single sperm with the egg plasma membrane initiates a wave of cortical granule exocytosis which begins at the site of sperm entry and propagates around the entire egg (Grey et al., 1974; Hara and Tydeman, 1979). Contents of the cortical granules, including enzymes and structural proteins, are released into the PS where they interact with the ECM to produce a functionally altered fertilization envelope (Grey et al., 1974; Wolf, 1974; Gerton and Hedrick, 1986). These alterations are complete by ~15–20 min after sperm penetration and result in a structural block to polyspermy (Grey et al., 1976).

Two major biochemical modifications in the ECM of *Xenopus* eggs at fertilization have been described. The first change is the formation of an electron-dense fertilization (F) layer at the interface of the VE and the innermost jelly coat (J1) (Grey et al., 1974; Wolf, 1974). This layer is formed from the calcium-dependent precipitation of a cortical granule lectin with components of J1 (Wyrick et al., 1974; Greve and Hedrick, 1978). The second modification in the matrix

Carolyn A. Larabell's present address is Hopkins Marine Station, Stanford University, Pacific Grove, CA 93950.

1. *Abbreviations used in this paper*: ECM, extracellular matrix; F layer, fertilization layer; J1, innermost jelly coat; MV, microvilli; PS, perivitelline space; S layer, smooth layer; VE, vitelline envelope.

is a decrease in molecular mass of two glycoproteins in the VE (69 to 66 kD and 64 to 61 kD) due to a limited hydrolysis reaction (Gerton and Hedrick, 1986). Thin-section EM, however, has been unable to visualize significant ultrastructural changes accompanying this modification (Grey et al., 1974).

Here we report the three-dimensional organization of the ECM in unfertilized and fertilized *Xenopus* eggs as seen in platinum replicas of quick-frozen and deep-etched specimens. Using this technique, we demonstrate in great detail the multilayered nature of these extracellular investments and their structural modification at fertilization. In addition, we describe the structure of the smooth (S) layer, a complex surface coat surrounding the fertilized egg which has not been previously visualized.

Materials and Methods

Egg Procurement

Adult female *Xenopus* were purchased from Nasco Biological Supply Co. (Fort Atkinson, WI) and raised on a 12-h light/12-h dark cycle in recirculated, filtered 10% Holtfreter's solution. Females were injected with 900 IU human chorionic gonadotropin and eggs were collected 8–9 h later by stripping them from the frog. Eggs were stored in 1.5× O-R2 buffer (123.8 mM NaCl, 3.8 mM KCl, 1.5 mM $CaCl_2$, 1.5 mM $MgCl_2$, 1.5 mM Na_2HPO_4, 5.7 mM NaOH, 7.5 mM Hepes, pH 7.8; Hollinger and Corton, 1980) until used (maximum storage time was 1 h). Males were killed and testes removed, washed, and then macerated in 1.5× O-R2. Sperm were collected and stored in fresh 1.5× O-R2 until needed (maximum storage time was 4 h). Fertilization was carried out by addition of 100 μl of concentrated sperm to 6 ml of F-1 solution (41.25 mM NaCl, 1.25 mM KCl, 0.25 mM $CaCl_2$, 0.06 mM $MgCl_2$, 0.5 mM Na_2HPO_4, 1.9 mM NaOH, 2.5 mM Hepes, pH 7.8; Hollinger and Corton, 1980) containing 20–40 eggs; the final sperm concentration was 10^5–10^6 cells/ml (Hollinger and Corton, 1980). Success of fertilization was determined by allowing periodic samples to proceed to first cleavage.

Sample Preparation and EM

Both fixed and unfixed samples were used for quick-freezing. Samples that were fixed were incubated overnight at 4°C in 2.5% glutaraldehyde (dejellied eggs) or 5% glutaraldehyde (jellied eggs) in 45 mM s-collidine buffer, pH 7.6. To compare our results with those obtained previously by thin sectioning, some glutaraldehyde-fixed samples were subsequently washed in buffer (three times) and fixed in 1% OsO_4 in s-collidine buffer for 1 h. Unfixed and glutaraldehyde-fixed samples demonstrated comparable views, with only a slight decoration of filaments observed in fixed samples. Samples fixed in both glutaraldehyde and OsO_4 provided excellent views of the F layer but did not reveal the S layer. Presumably this layer must be osmium sensitive. All samples were dejellied before quick-freezing. Unfixed eggs and zygotes were chemically dejellied using 45 mM β-mercaptoethanol in F-1, pH 9.3, for 3–5 min or until all jelly visible in the dissecting microscope

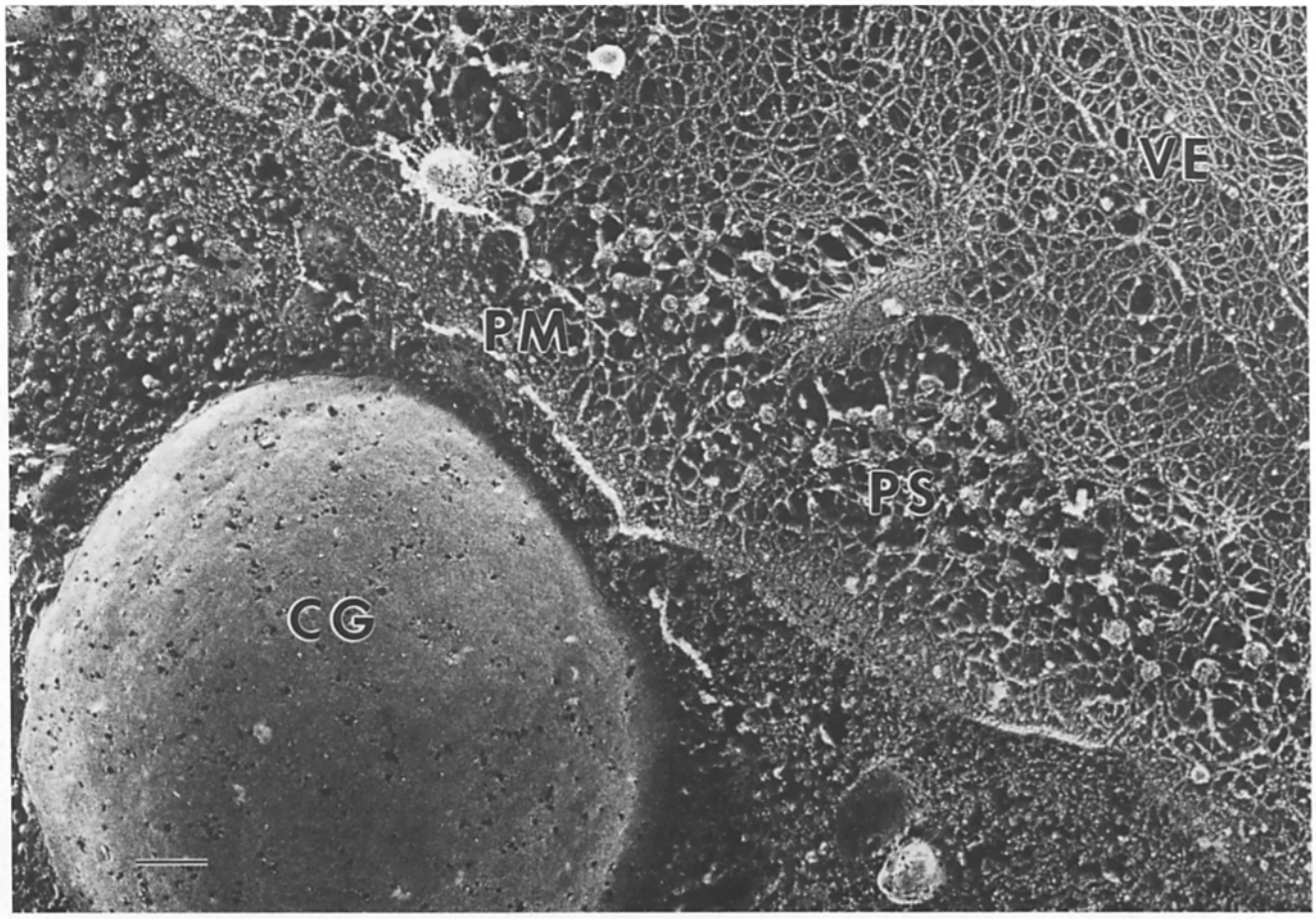

Figure 1. Electron micrograph of a platinum replica of an unfertilized *Xenopus* egg showing egg cortex, with large cortical granule (*CG*) just beneath the plasma membrane (*PM*), and overlying ECM. The ECM is composed of the PS and VE. The specimen was fixed in glutaraldehyde, mechanically dejellied, passed through distilled water, quick-frozen, freeze-fractured, deep-etched, and rotary-shadowed with platinum–carbon. This figure and all subsequent figures have been photographically reversed; platinum deposits appear white. Bar, 0.2 μm.

had been removed. Fixed samples were mechanically dejellied using Dumont No. 5 forceps. Excess salts were removed from fixed samples before quick-freezing by rinsing samples in F-1 solution (once) then in distilled H_2O (three times). Unfixed samples were rinsed in 0.5× F-1 to remove excess salts without exposing the living samples to osmotic stress. All specimens were quick-frozen on a liquid helium–cooled copper block using the apparatus designed by Heuser et al. (1979). Quick-frozen samples were then fractured in a Freeze-Etch Unit (model 400D, Balzers Corp., Hudson, NH) and allowed to etch at a temperature of −90°C for 8–12 min at a pressure of 10^{-6} mbar. The specimen was then rotary-shadowed with platinum–carbon applied from an electron gun positioned at 25° and the replica backed with carbon applied from an angle of 75°. Replicas were cleaned in 5% so-

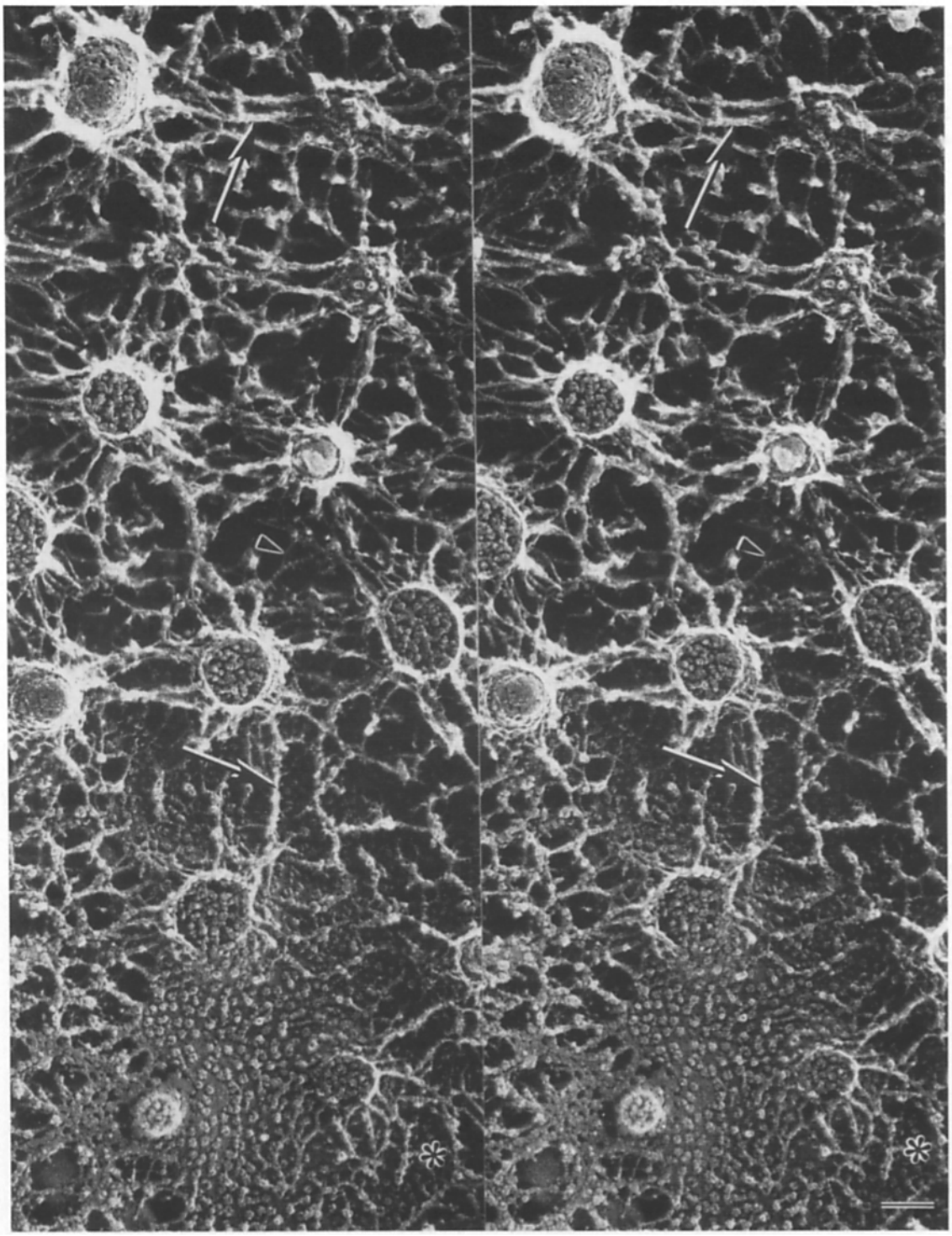

Figure 2. Oblique fracture through the PS of an unfertilized egg with exposed plasma membrane at the bottom of the micrograph. MV protruding from the plasma membrane have been fractured open at increasingly higher levels from bottom to top. Oblique fibers (*arrows*) can be seen extending from the MV to the egg surface as well as to adjacent MV; short, fine filaments (*arrowheads*) interconnect these fibers. Intermediate-sized fibrils (*asterisks*) are seen running between particles on the plasma membrane. Specimen was prepared as described in Fig. 1. Stereo pair shown. Bar, 0.1 μm.

dium hypochlorite (60°C) for 1 h, followed by 70% sulfuric acid (60°C) for 1 h, and then 5% sodium hypochlorite again (60°C) for 1 h, with a rinse in distilled H_2O between each transfer. Replicas were viewed at 80 kV in a microscope (model EM 300, Philips Electronic Instruments, Inc., Mahwah, NJ). Stereo images were obtained using a eucentric goniometer stage; the specimen was tilted ±9°. All figures are presented as negative images so that platinum deposits appear white. Platinum replica thickness averaging 1.6 nm is included in the measurements of filament diameter. These are reported as means ± SD in the results section.

Results

Replicas of quick-frozen, deep-etched *Xenopus* eggs provide a three-dimensional view of the ECM before and after fertilization. A cross fracture through the cortex of an unfertilized *Xenopus* egg illustrates the matrix, including the PS and VE, attached to the egg surface (Fig. 1). A large cortical granule lies just under the plasma membrane. The PS between the plasma membrane and the overlying VE is filled with a complex network of filaments. This network is visualized best in stereo micrographs of grazing fractures. In Fig. 2, an oblique fracture has exposed the external surface of the plasma membrane (at the bottom of the micrograph) and microvilli (MV) protruding into the PS. From the bottom of the figure to the top, MV have been cross fractured at increasingly higher levels revealing the network of filaments within. A complex glycocalyx lies within the extracellular space and interconnects these MV with at least three populations of fibers. The first and largest population consists of oblique fibers which connect microvillar tips with the plasma membrane below, almost appearing like "guy wires" (*arrow*, Fig. 2). These fibers also run from one microvillar tip to another and join other guy wires midcourse. Oblique fibers are heterogeneous in size, ranging from 6.5 to 16 nm in diameter (10.4 ± 2.7 nm; mean ± SD, n = 55). A second population of fibers in the PS consists of short, fine filaments (4.0 ± 0.6 nm in diameter, n = 35) which interconnect the oblique fibers described above (*arrowheads*, Fig. 2). These are not as abundant, but are consistently observed. Finally, a third population of short fibrils (9.6 ± 1 nm in diameter, n = 35) interconnects small particles located on the external surface of the plasma membrane (*asterisk*, Fig. 2). These three populations form an elaborate network which fills the entire PS.

Numerous membrane-bound vesicles, ranging from 40 to 110 nm in diameter (60 ± 13 nm; mean ± SD, n = 60), are also seen in the PS just under the VE (Fig. 3). Each vesicle is in contact with several of the fibrils coursing through the PS, making them an integral component of the filamentous network. Vesicles, when fractured, reveal that they are membrane bound and are filled with a globular material. The fibrils of the PS network, which interconnect the vesicles and MV, are continuous with the fibers of the overlying VE (Fig. 3).

The VE, at its innermost surface, is attached to the tips of the MV via a layer of horizontal filaments (*HF*, Fig, 3). The horizontal filaments that orbit the egg at the PS/VE interface represent an ultrastructurally distinct sublayer within the VE. This layer is composed of tightly packed fibrils (10 ±

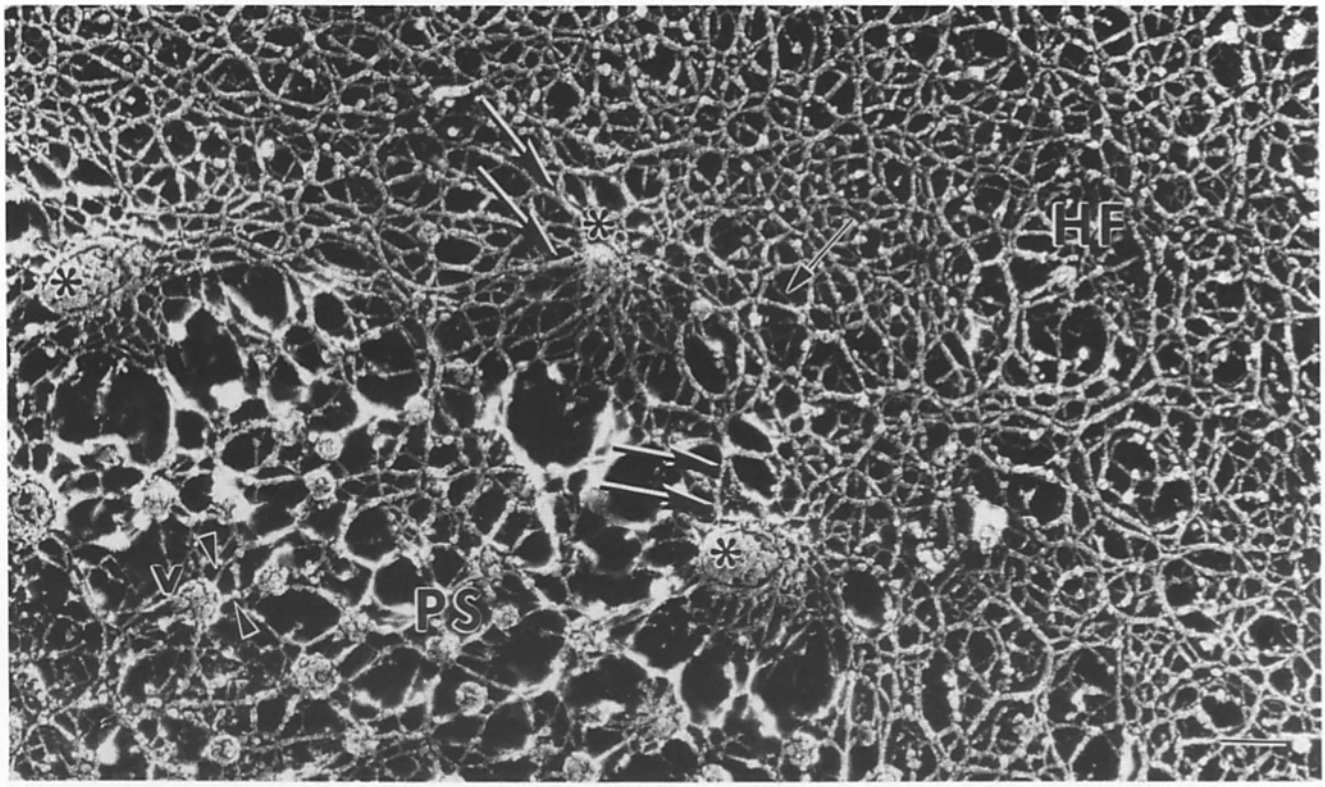

Figure 3. Oblique fracture of the junction between the PS and overlying VE. The PS contains numerous membrane-bound vesicles (*v*), each of which is contacted by several fibrils (*arrowheads*). The inner portion of the VE consists of a dense meshwork of horizontal filaments (*HF*) which are interconnected by short thin filaments (*small arrows*). The tips of MV (*asterisks*), seen just beneath the VE, are attached to the horizontal filament fibrils (*large arrows*). Specimen was prepared as described in Fig. 1. Bar, 0.1 μm.

1.3 nm in diameter, $n = 60$) which are highly interconnected. Linking these fibrils are short, thin filaments ~4.6 ± 0.5 nm ($n = 35$) in diameter.

The remainder of the VE is of a clearly different architecture. Its structure is dominated by large, cable-like fibers (19 ± 1.6 nm in diameter, $n = 35$) which run throughout the envelope, often in a swirling fashion. Individual fibers can be followed for long distances as they twist and turn, often converging to form bundles (*asterisk*, Fig. 4) as well as bifurcating into smaller fibrils. A second population of fibrils, intermediate in size (12 ± 1.6 nm in diameter, $n = 40$), are also observed coursing throughout the VE in a tangled fashion. These fibrils often bifurcate into two fibrils which then proceed in different directions. These two major sets of cable-like fibers are cross-linked by fine, short filaments (5.1 ± 0.7 nm in diameter, $n = 35$) at random locations.

The ECM of the unfertilized egg is dramatically altered after fertilization in three distinct ways: formation of a smooth, multilayered envelope at the PS/VE interface, conversion of the VE to an altered VE, and formation of the F layer at the altered VE/J1 interface. All three modifications appear to result from interactions of the VE and jelly coat with enzymes and structural material released by cortical granule exocytosis. Two of the cortical granule enzymes are believed to be proteases responsible for the cleavage of the 69- and 64-kD components of the VE to the 66- and 61-kD components of the altered VE (Gerton and Hedrick, 1986). In addition, a large metalloglycoprotein (a 539/655-kD doublet) released from the cortical granules binds at the VE/J1 interface in a lectin/ligand reaction to form a band of precipitation, the F layer (Grey et al., 1974; Wolf, 1974; Wyrick, et al., 1974; Greve and Hedrick, 1978).

Deposition of an S layer of material on the tips of the MV at the PS/VE interface (Figs. 5–7) is seen within 10 min after insemination. This structure is deposited in a patchwork fashion at early times (Fig. 5) and by 15 min after insemination, the entire egg is surrounded by a very thin, multilaminar envelope. The extremely smooth outer surface of this investment suggests our designation: the S layer. The S layer is actually composed of two tightly apposed sheets which can be clearly distinguished at higher magnification. The innermost sheet (*FS*, Fig. 7) manifests a fibrous nature and splays

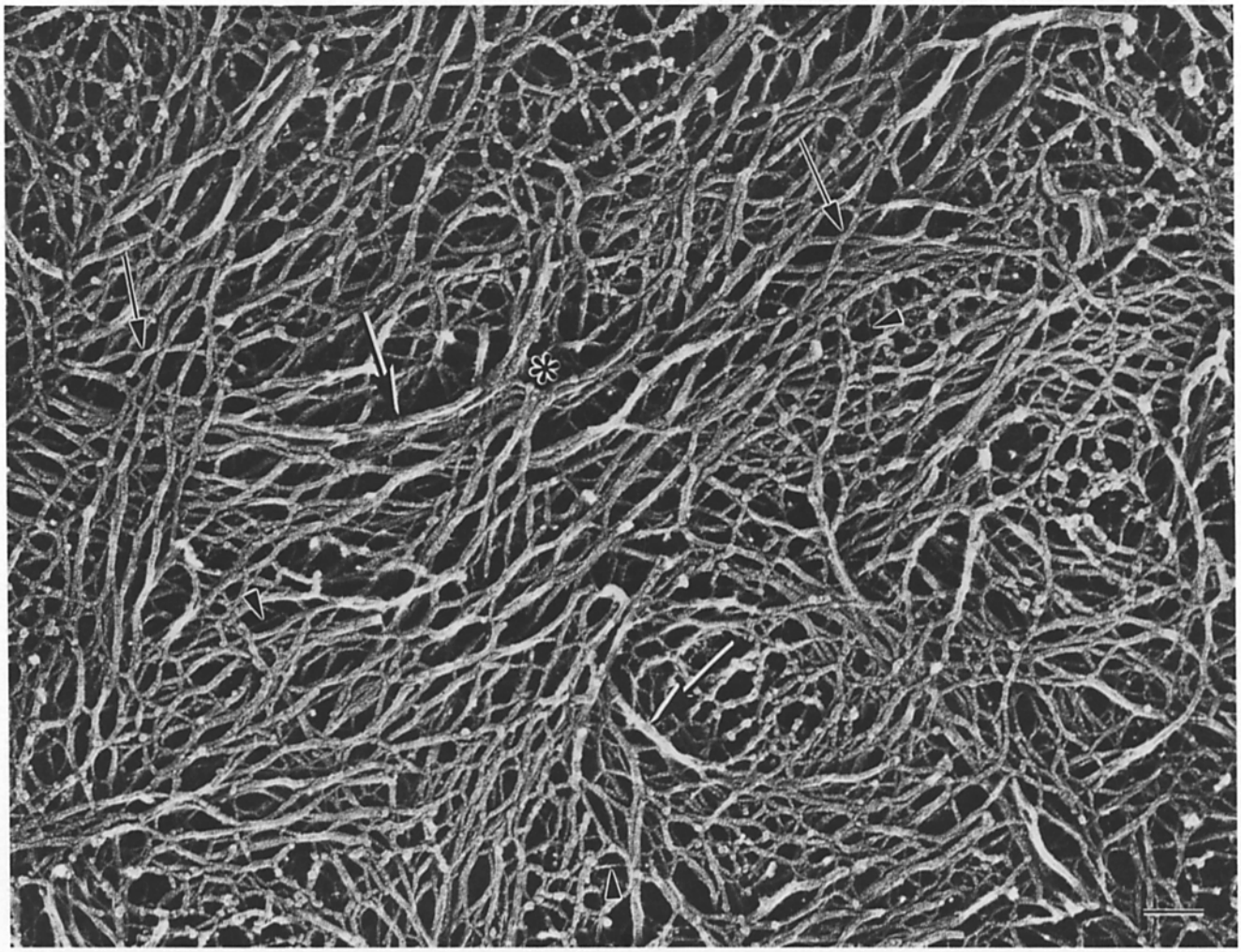

Figure 4. The VE of the unfertilized egg (outer portion). Large cable-like fibers (*thick arrows*) run for long distances and occasionally form bundles (*asterisk*). Intermediate-sized fibrils also course throughout the VE, frequently bifurcating (*thin arrows*). Small, fine filaments interconnect the larger fibers and fibrils (*arrowheads*). Specimen was chemically dejellied, quick-frozen without fixation, and freeze-fractured as described in Fig. 1. Bar, 0.1 μm.

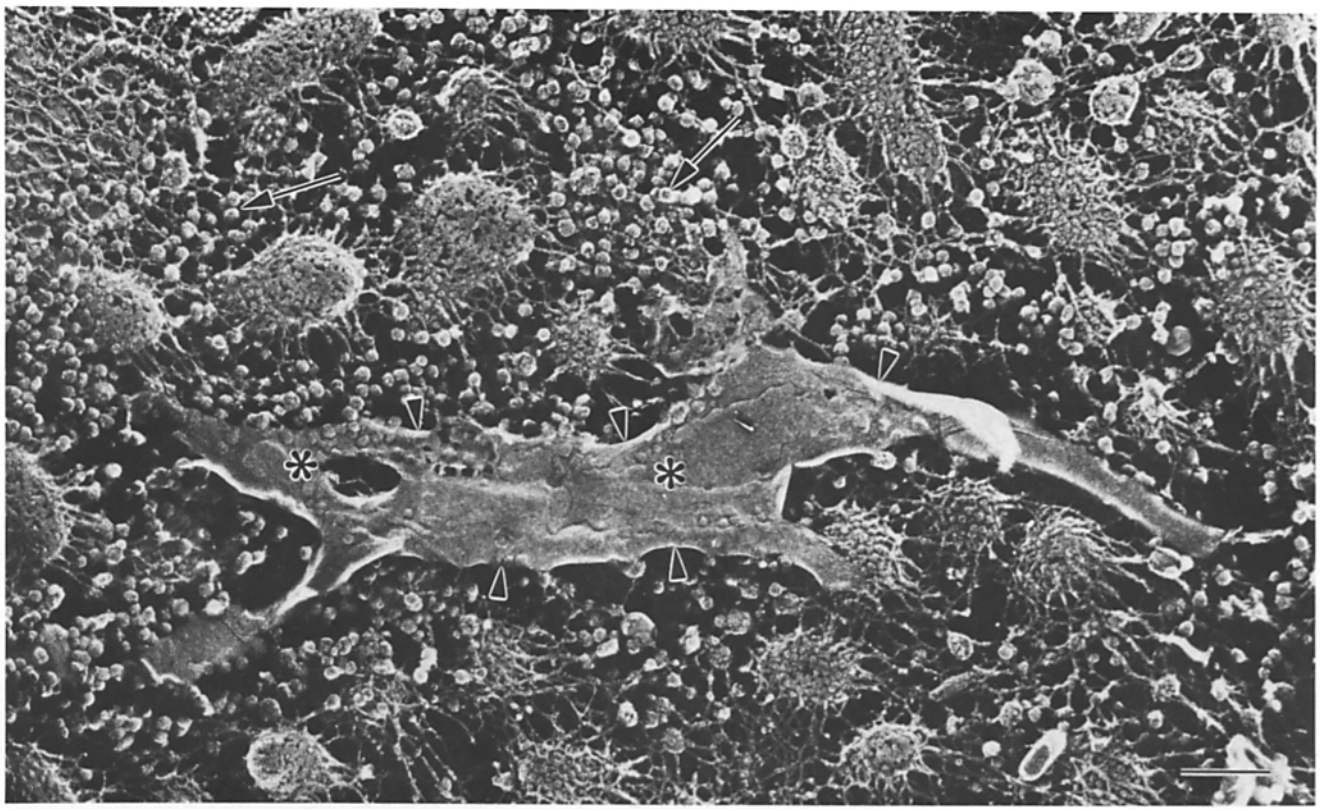

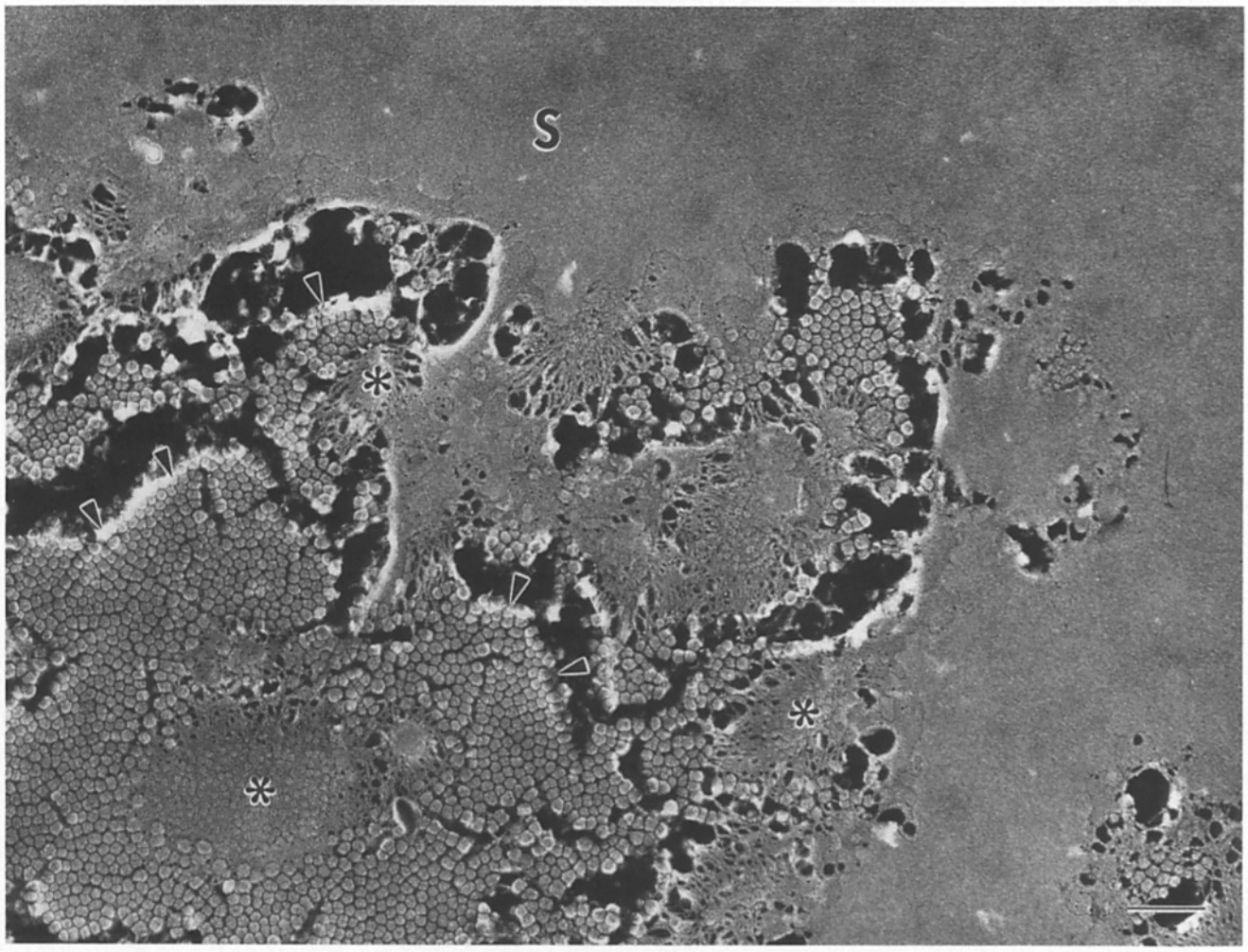
S

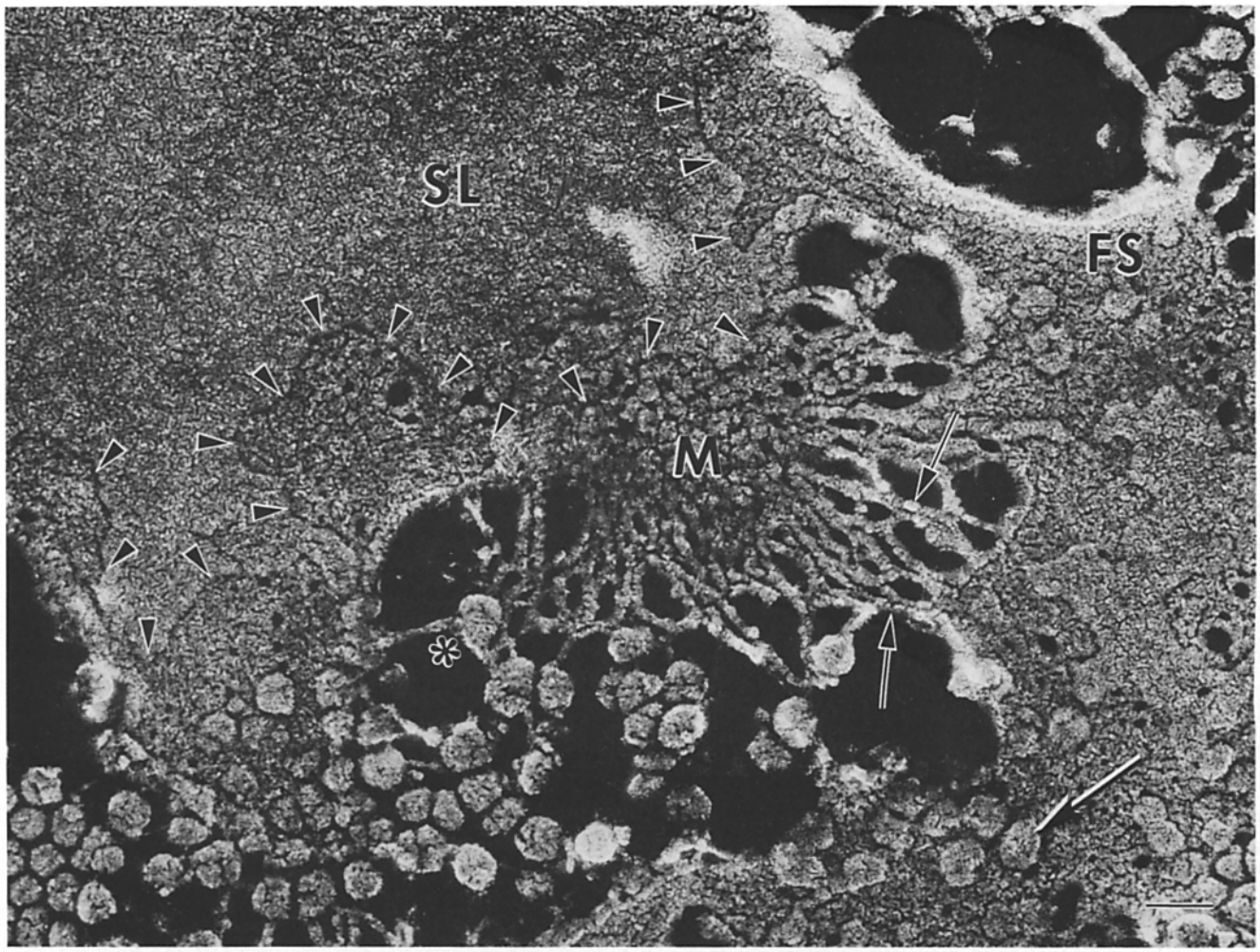

Figure 7. High magnification view of the S layer demonstrating its multilayered appearance. The innermost sheet is fibrous and can be seen splaying into filaments (*small arrows*) which attach to MV tips (*M*) and to the small particles nearby (*asterisks*). Clusters of these particles have become enmeshed in this fibrous sheet (*large arrow*). The smooth outer layer (*SL*) lies directly on top of the fibrous sheet (*FS*) and is separated by a line of demarcation (*arrowheads*). Specimen was prepared as described in Fig. 6. Bar, 50 nm.

into filaments (9 ± 1.6 nm diameter, $n = 60$) that attach to the tips of the MV (*small arrows*, Fig. 7). Directly on top of, and largely covering this layer, is a material that is completely smooth within the resolution of our platinum shadowing (*SL*, Fig. 7). During formation of the S layer, large numbers of small particles (36 ± 4.9 nm in diameter, $n = 75$) are observed in the PS in addition to the patches of S layer material (*arrows*, Fig. 5). These particles often aggregate in large plaques around the tips of the MV (*arrowheads*, Fig. 6) and several of these small particles are seen enmeshed in the innermost fibrous sheet (*large arrow*, Fig. 7). The S layer demonstrates no attachments to the overlying altered VE.

The VE itself, lying above the S layer, is transformed within 5 min after insemination from a network of loosely woven, cable-like fibers to an arrangement of multiple concentric fibrous sheets, the altered VE (Fig. 8 *a*). These sheets often twist and curl to contact adjacent layers, forming a structure reminiscent of Baklava, or puff pastry. At higher magnification (Fig. 8 *b*), each sheet appears fibrous in texture, with numerous filaments (10 ± 2.3 nm in diameter, $n = 60$) emanating from each sheet to contact neighboring sheets.

The third modification consists of formation of the F layer at the altered VE/J1 interface. In cross fracture of quick-

Figure 5. (*Top*) Aerial view of the PS ~10 min after insemination. Numerous small particles are present at this time (*arrows*). The S layer has started to form in small patches (*arrowheads*) on the tips of the MV. Asterisks point out particle inclusions within the S layer. Specimen was chemically dejellied 10 min after insemination, fixed in glutaraldehyde, then quick-frozen and freeze-fractured as described in Fig. 1. Bar, 0.2 μm.

Figure 6. (*Bottom*) Aerial view of the S layer during its formation. The completely formed S layer is entirely smooth, as seen in the upper portion of the micrograph. Tips of several MV (*asterisks*) can be seen with plaques of small particles surrounding them (*arrowheads*). Specimen was chemically dejellied 13 min after insemination, fixed in glutaraldehyde, then quick-frozen and freeze-fractured as described in Fig. 1. Bar, 0.2 μm.

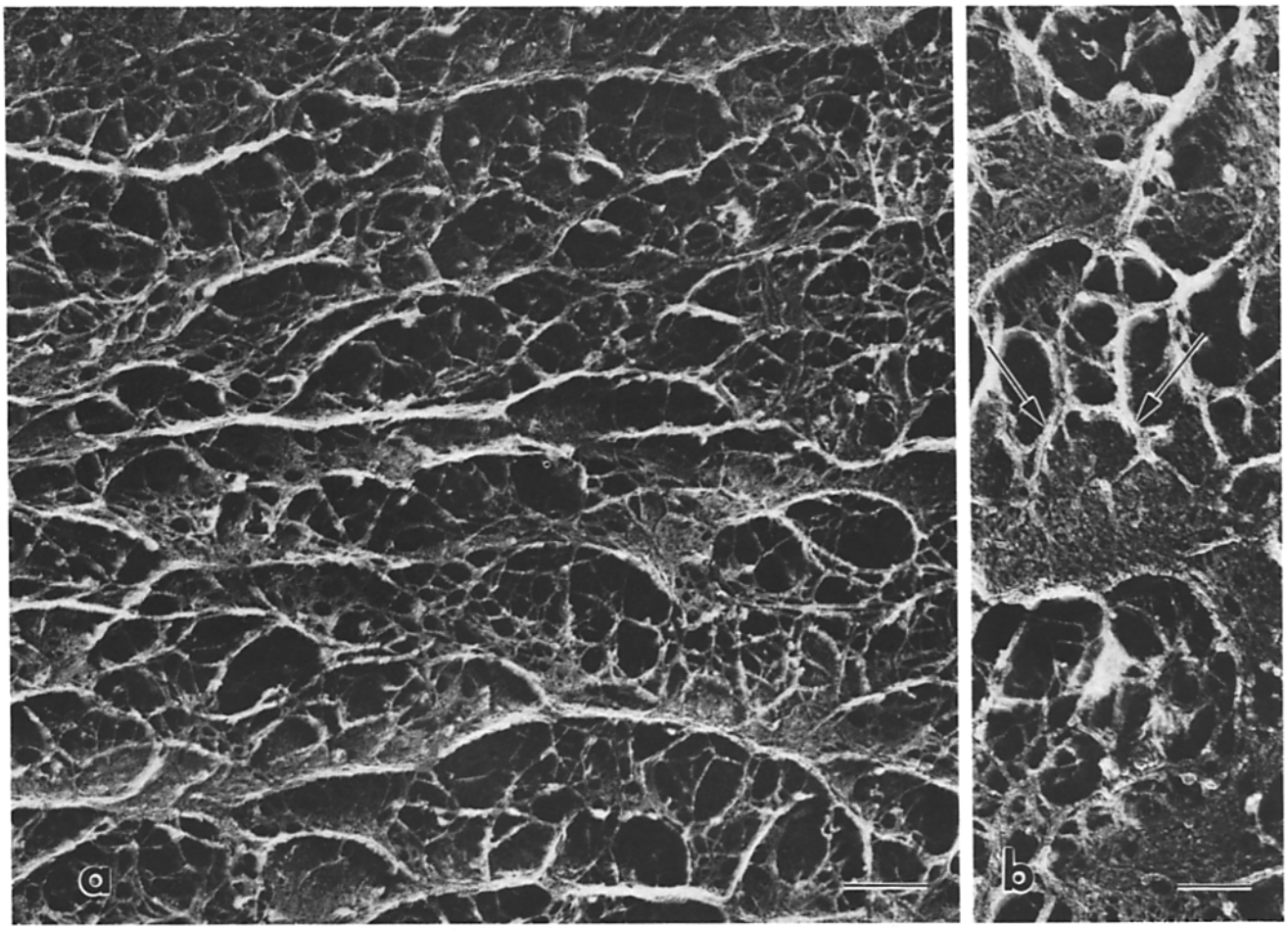

Figure 8. (*a*) Cross section of altered VE demonstrating the concentric fibrous sheets seen after fertilization. (*b*) Higher magnification view of the sheets demonstrating their fibrous nature. Arrows point to fibers emanating from a sheet and interconnecting adjacent shelves. Sample was fixed in glutaraldehyde 10 min after insemination, mechanically dejellied, then prepared for quick-freezing and freeze-fracture as described in Fig. 1. Bars: (*a*) 0.2 μm; (*b*) 0.1 μm.

frozen and deep-etched eggs, the F layer appears as a particle-decorated sheet segregating the altered VE below from the jelly coat above (Fig. 9 *a*). This band of precipitation is divided into two components, the condensed and dispersed components, as previously seen in thin sections (Grey et al., 1974). At higher magnification (Fig. 9 *b*), the F condensed component appears as a layer of small, tightly compacted particles at the outermost surface of the altered VE, while the F dispersed component consists of numerous short fibrils arranged in a "briar patch" fashion. These filaments appear to be decorated with particles similar to those in the F condensed layer. At regular intervals the F layer material, including both condensed and dispersed components, forms fingers which invaginate into the underlying altered VE. Short filaments are observed attaching the F layer material to the surrounding altered VE (*arrows*, Fig. 9 *c*).

Discussion

The quick-freeze, deep-etch, rotary-shadow technique has allowed us to report the structure of vertebrate egg investments at a level of complexity not previously achieved. The structure of most ECMs as seen in thin section is limited due to two problems: inadequate staining of filament networks and lack of three-dimensional information. The VE of the *Xenopus laevis* egg is no exception. In thin sections it appears as a 1-μm-thick layer of nondescript filaments which, after fertilization, elevates from the egg surface and becomes

Figure 9. (*a*) Cross section of the F layer at the altered VE/J1 interface. The F condensed (F_c) component is innermost, lying immediately on top of the VE, and the F dispersed (F_d) component extends from it. F layer material often invaginates into the underlying VE (*arrows*). (*b*) Higher magnification view of the F layer demonstrating the tightly compacted particles of the F condensed component (*arrows*) and filamentous attachments between the F layer and altered VE (*arrowheads*). The F dispersed component above is a briar patch of short fibers decorated with particles. (*c*) Invagination of F layer material into the VE (cross-sectional view). Arrows point to attachment sites between the F layer and surrounding VE. Samples in *a* and *b* were chemically dejellied, fixed in glutaraldehyde and OsO_4, and then prepared for quick-freezing and freeze-fracture as described in Fig. 1. Sample in *c* was chemically dejellied and quick-frozen without fixation and then freeze-fractured as described in Fig. 1. Bars: (*a* and *c*) 0.2 μm; (*b*) 0.1 μm.

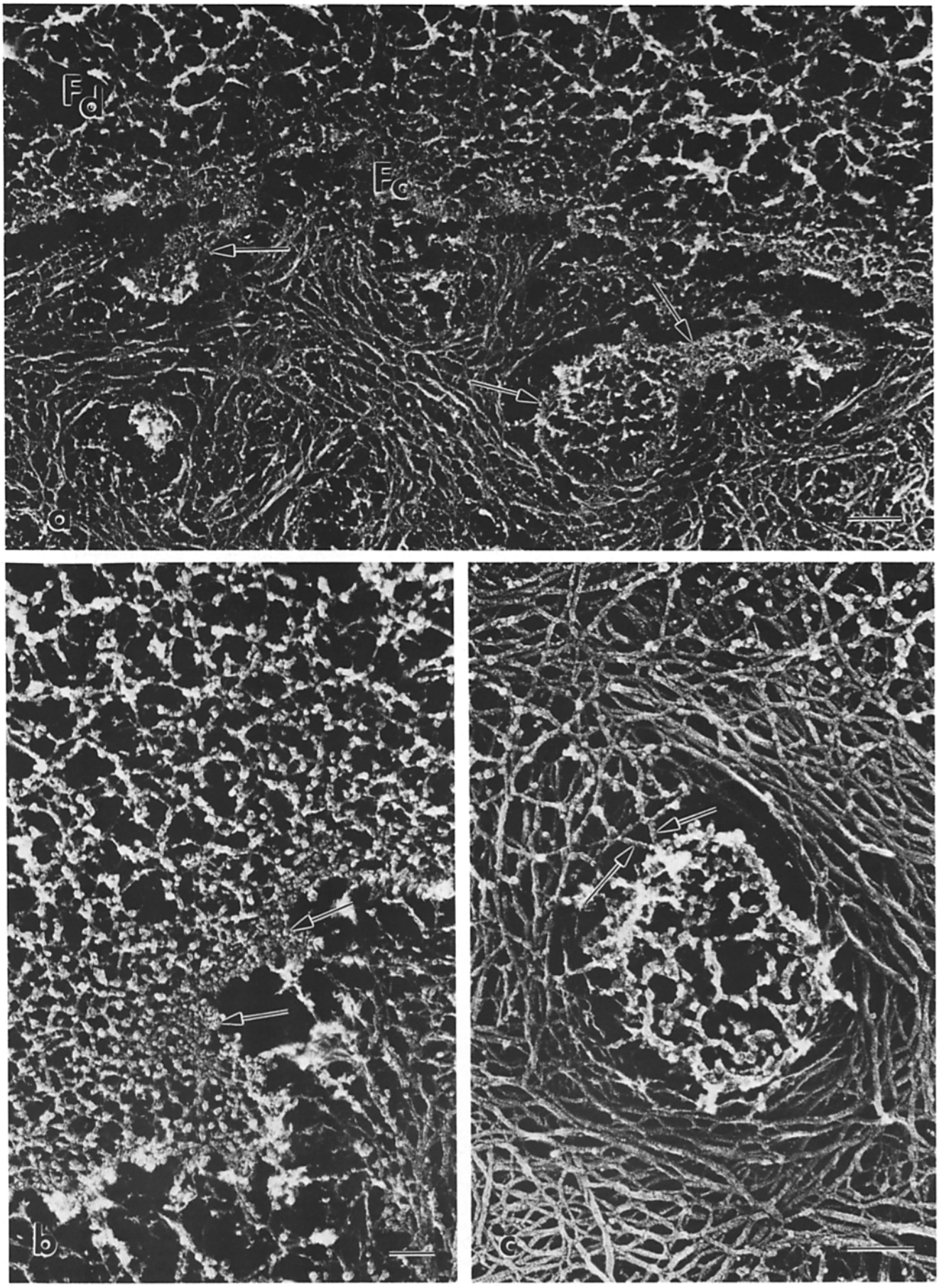
Fd
Fc
a
b
c

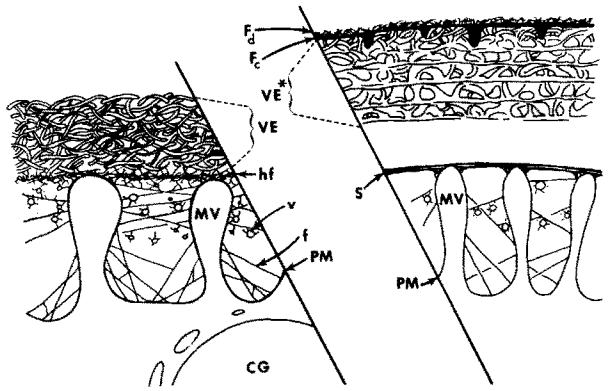

Figure 10. Diagram of the ECM of the *Xenopus* egg before and after fertilization. The unfertilized egg (*left side*) with a cortical granule (*CG*) beneath the plasma membrane *PM* and MV extending into the PS. Filaments (*f*) connect MV to each other, to the plasma membrane, and to vesicles (*v*) seen in this region. The VE lies on the tips of the MV and is attached to the MV by a layer of horizontal filaments (*hf*) seen at the innermost portion of the VE. After fertilization (*right side*), the S layer (*S*) encircles the egg, lying on the tips of the MV. The VE has elevated and has been chemically and structurally altered (*VE**); the F layer (F_d and F_c) has been deposited on the outer surface of the altered VE.

Table I. Components of ECM around Xenopus Eggs before and after Fertilization

Unfertilized	Diameter*	Fertilized	Diameter
	nm		*nm*
PS filaments		PS filaments	ND
Oblique	10 ± 2.7		
On PM	10 ± 1.2		
Small	4 ± 0.6	S layer	
HF filaments		Particles	36 ± 4.9
Medium	10 ± 1.3	Filaments	9 ± 1.6
Small	5 ± 0.5	Altered VE filaments	
VE filaments		(between sheets)	
Large	19 ± 1.6	Medium	10 ± 2.3
Medium	12 ± 1.6	Small	4 ± 0.8
Small	5 ± 0.7	Altered VE filaments	
		(below F layer)	
		Medium	10 ± 3
		Small	4 ± 1

* Diameter measurements include platinum replica thickness; platinum thickness averaged 1.6 nm overall but may have varied locally. Measurements were made from replicas of three different samples.

coated with an electron-dense band of precipitation, but otherwise appears to undergo little ultrastructural change.

In contrast, the deep-etching method we have used shows that the ECM of the unfertilized egg is a complex, multilayered envelope whose structure and filament composition is summarized in Fig. 10 and Table I, respectively. The VE itself consists of two separate layers—an inner layer of horizontal filaments (*hf*, Fig. 10) and an outer, thicker layer of curling, cable-like fibers (*VE*, Fig. 10). These horizontal filaments are attached to the microvillar tips below and at numerous points become continuous with filaments in the PS. Beneath the VE is an elaborate glycocalyx (*f*, Fig. 10) that fills the PS. The glycocalyx is complex, but consists chiefly of oblique filaments that link microvillar surfaces with the plasma membrane below and numerous membrane-bound vesicles which are an integral component of this filamentous network (*v*, Fig. 10).

Unlike previous thin-section data, our work demonstrates that the VE structure is securely linked to PS filaments and the egg surface below as well as to the J1 above (data not shown). It is not surprising, then, that when these eggs are oviposited, the sticky jelly affixes to a substrate and consequently determines the orientation of the egg, which is often different than that expected based on gravity alone (i.e., heavier, vegetal hemisphere downward).

At fertilization, elaborate modification of the ECM is observed. Platinum replicas of deep-etched eggs show that the VE undergoes profound structural changes that cannot be seen in thin sections. The array of large cable-like fibers is transformed into concentric fibrous sheets; the fibers that emanate from these sheets to connect adjacent shelves are similar in diameter to the medium- and small-diameter filaments seen in the VE before fertilization (Table I). In addition, the F layer (F_c and F_d, Fig. 10), previously seen in thin sections as an electron-dense band of material at the altered VE/J1 interface (Grey et al., 1974), is actually a plate of tightly compacted small particles. The F layer appears to be anchored to the altered VE by invaginations of this material as well as by numerous short fibers (Fig. 9, *a* and *b*); together these structures constitute the fertilization envelope. These modifications could be those which convert the ECM from a structure which is receptive to sperm before fertilization to one which prevents additional sperm from contacting the egg surface after fertilization.

Our most striking discovery, however, is the presence of the S layer, a coating at the PS/VE interface that has not been previously identified. This extremely thin, multilayered envelope, which completely encompasses the egg by 15 min after insemination, orbits at the level of the microvillar tips. It is attached to the underlying MV by its innermost component, which is fibrous in nature, but is completely smooth at its outermost surface. No attachments are seen between the S layer and the overlying altered VE. This means that the filamentous connections seen between MV tips and overlying VE in the unfertilized egg have been severed. The fertilized egg is now completely unrestrained within the elevated altered VE. Soon after completion of the S layer, the egg rotates within the altered VE with respect to gravity, positioning the animal pole upward (Palacek et al., 1978; Hara and Tydeman, 1979). Gravitational orientation is known to be important for proper dorsal–ventral axis formation; if such orientation is prevented, abnormal embryos develop (Gerhart et al., 1981). Although not yet proven, formation of the S layer could act as a near-frictionless coating to facilitate rotation of the egg against the altered VE and jelly.

We believe the S layer, like the altered VE and F layer, is derived from contents of the cortical granules since its formation can be induced by the addition of cortical granule exudate to unfertilized eggs (Larabell, C. A., and D. E. Chandler, manuscript in preparation). The manner in which it is formed is not yet clear. One clue is that numerous small particles ~35 nm in diameter are seen at the PS/VE interface coincident with the appearance of small patches of the S layer material. In addition, these particles aggregate in plaques around microvillar tips (Fig. 6) and are found embedded in

the innermost filamentous sheet of this structure (Fig. 7), suggesting that they play some role in S layer formation.

The S layer can now be visualized, but its role in early development remains to be assessed. This layer may play a part in allowing orientation of the egg after fertilization as suggested above. Alternatively, it may play a direct role in the block to polyspermy. Stewart-Savage and Grey (1987) have shown that fertilized eggs cannot be reinseminated even after the fertilization envelope is stripped away. This suggests that there may be an additional surface layer that is not stripped off which particpates in the block. Indeed, these authors have shown that there is such a layer at the tips of the MV that can be seen only after labeling with cationic ferritin (Grey, R. D., personal communication). Future experiments should show whether this layer is equivalent to the S layer we see in deep-etched and rotary-shadowed specimens.

We thank Dr. Robert Grey for helpful discussions of his unpublished data.

This study was supported by grants from the National Science Foundation (DCB-8407152) and the National Institutes of Health (1K04-HD00619).

Received for publication 24 February 1988, and in revised form 4 April 1988.

References

Barros, C., and R. Yanagimachi. 1971. Induction of zona reaction in golden hamster eggs by cortical granule material. *Nature (Lond.).* 233:268–269.

Barros, C., and R. Yanagimachi. 1972. Polyspermy-preventing mechanisms in the golden hamster egg. *J. Exp. Zool.* 180:251–266.

Bleil, J. D., and P. M. Wassarman. 1980. Mammalian sperm-egg interaction: identification of a glycoprotein in mouse egg zona pellucida possessing receptor activity for sperm. *Cell.* 20:873–882.

Chandler, D. E., and J. Heuser. 1980. The vitelline layer of the sea urchin egg and its modification during fertilization. *J. Cell Biol.* 84:618–632.

Gerhart, J., G. Ubbels, S. Black, K. Hara, and M. Kirschner. 1981. A reinvestigation of the role of the grey crescent in axis formation in *Xenopus laevis*. *Nature (Lond.).* 292:511–516.

Gerton, G. L., and J. L. Hedrick. 1986. The vitelline envelope to fertilization envelope conversion in eggs of *Xenopus laevis*. *Dev. Biol.* 116:1–7.

Glabe, C. G., and V. D. Vacquier. 1978. Egg surface glycoprotein receptor for sea urchin sperm bindin. *Proc. Natl. Acad. Sci. USA.* 75:881–885.

Greve, L. C., and J. L. Hedrick. 1978. An immunocytochemical localization of the cortical granule lectin in fertilized and unfertilized eggs of *Xenopus laevis*. *Gamete Res.* 1:13–18.

Grey, R. D., D. P. Wolf, and J. L. Hedrick. 1974. Formation and structure of the fertilization envelope in *Xenopus laevis*. *Dev. Biol.* 36:44–61.

Grey, R. D., P. K. Working, and J. L. Hedrick. 1976. Evidence that the fertilization envelope blocks sperm entry in eggs of *Xenopus laevis*: interaction of sperm with isolated envelopes. *Dev. Biol.* 54:52–60.

Hara, K., and P. Tydeman. 1979. Cinematographic observation of an "activation wave" (AW) on the locally inseminated egg of *Xenopus laevis*. *Wilhelm Roux's Arch. Dev. Biol.* 186:91–94.

Heuser, J. E., T. S. Reese, M. J. Dennis, Y. Jan, L. Jan, and L. Evans. 1979. Synaptic vesicle exocytosis captured by quick-freezing and correlated with quantal transmitter release. *J. Cell Biol.* 81:275–300.

Hollinger, T. G., and G. L. Corton. 1980. Artificial fertilization of gametes from the South African clawed frog, *Xenopus laevis*. *Gamete Res.* 3:45–57.

Palacek, J., G. A. Ubbels, and K. Rzehak. 1978. Changes of the external and internal pigment pattern upon fertilization in the egg of *Xenopus laevis*. *J. Embryol. Exp. Morphol.* 45:203–214.

Rossignol, D. P., B. J. Earles, G. L. Decker, and W. J. Lennarz. 1984. Characterization of the sperm receptor on the surface of eggs of *Strongylocentrotus purpuratus*. *Dev. Biol.* 104:308–321.

Stewart-Savage, J., and R. D. Grey. 1987. Loss of functional sperm entry into *Xenopus* eggs after activation correlates with a reduction in surface adhesivity. *Dev. Biol.* 120:434–446.

Veron, M., C. Foerder, E. M. Eddy, and B. M. Shapiro. 1977. Sequential biochemical and morphological events during assembly of the fertilization membrane of the sea urchin. *Cell.* 10:321–328.

Wolf, D. P. 1974. The cortical granule reaction in living eggs of the toad, *Xenopus laevis*. *Dev. Biol.* 36:62–71.

Wolf, D. P., T. Nishihara, D. M. West, R. E. Wyrick, and J. L. Hedrick. 1976. Isolation, physicochemical properties, and the macromolecular composition of the vitelline and fertilization envelopes from *Xenopus laevis* eggs. *Biochemistry.* 15:3671–3678.

Wyrick, R. E., T. Nishihara, and J. L. Hedrick. 1974. Agglutination of jelly coat and cortical granule components and the block to polyspermy in the amphibian *Xenopus laevis*. *Proc. Natl. Acad. Sci. USA.* 71:2067–2071.